Photoemission and scanning-tunneling-microscopy study of GaSb(100)

G. E. Franklin, D. H. Rich, A. Samsavar, E. S. Hirschorn, F. M. Leibsle,
T. Miller, and T.-C. Chiang
Department of Physics, University of Illinois at Urbana-Champaign, 1110 West Green Street, Urbana, Illinois 61801
and Materials Research Laboratory, University of Illinois at Urbana-Champaign,
104 South Goodwin Avenue, Urbana, Illinois 61801
(Received 8 February 1990)

Angle-resolved and angle-integrated synchrotron-radiation photoemission together with scanning tunneling microscopy (STM) were used to study the Sb-stabilized GaSb(100)-(1×3) surface grown by molecular-beam epitaxy. Bulk valence bands were mapped out in the Γ-Δ-*X* direction. The deconvoluted Sb 4*d* and Ga 3*d* core-level line shapes were used to construct a structural model for the surface. STM resolved the individual atomic dimers verifying the proposed model and showed partial disorder inherent on this surface.

I. INTRODUCTION

Over the past decade there has been considerable interest in the growth and electronic structure of III-V compound semiconductors. By using the techniques of molecular-beam epitaxy (MBE), high-quality samples can be prepared and various surface reconstructions can be fabricated which determine the electronic states and chemical properties of the surface. These surface reconstructions depend not only on the surface orientation of the crystal but also on the growth conditions. Emphasis has been placed on GaAs for its obvious technological use. However, in order to understand the nature of these zinc-blende-structure systems, other III-V compounds are equally important. Towards this end, we decided to study the GaSb(100) surface, which is technologically important in its own right (i.e., tunneling diodes, heterostructure lasers, etc.),[1] and which can help as a comparative study with other (100) III-V surfaces such as GaAs and InSb.

This work is a study of the GaSb(100) surface using high-energy electron diffraction (HEED), synchrotron-radiation photoemission spectroscopy, and scanning tunneling microscopy (STM). HEED patterns were used to assess the long-range periodicity and quality of the surface. The basic electronic, chemical, and structural properties of the surface were evaluated by using angle-resolved photoemission to determine band structure, by using angle-integrated photoemission to observe the Ga 3*d* and Sb 4*d* core-level line shapes, and by STM giving us high-resolution images of surface structure. By combining these results and showing consistency among them, a detailed picture of the GaSb(100) surface is determined.

II. EXPERIMENTAL DETAILS

Our *n*-type, Te-doped GaSb(100) samples (carrier density 1.5×10^{17} cm^{-3}) were purchased from MCP Electronic Materials (England). The samples were aligned by Laue diffraction to within 0.5°. Alumina powder was used for the initial rough polishing. Samples were then mechanochemically polished to a mirror finish with Cab-O-sperse, a colloidal slurry purchased from Rippey (Santa Clara, CA). For a quicker polish the *p*H was changed from 5.5 to 9 using ammonia. The clean polished GaSb(100) sample was placed in the vacuum chamber, with pressures better than 1×10^{-10} Torr, and was heated via direct current. Several cycles of argon-ion sputtering with 500-eV ions and annealing at 500 °C were enough to obtain clean, ordered (1×3) surfaces which were used as starting surfaces for MBE growth. Auger spectroscopy determined the cleanliness of the sample. MBE was accomplished through evaporation from electron-beam heated crucibles containing 99.999% purity Ga and Sb. The rate of deposition for each material was monitored using a water-cooled quartz-crystal thickness monitor. In this paper 1 monolayer (ML) of Ga or Sb is defined as 5.38×10^{14} atoms/cm^2, which is the site-number density for the unreconstructed GaSb(100) surface.

Photoemission experiments were conducted at the Synchrotron Radiation Center (Stoughton, WI) of the University of Wisconsin–Madison on the 1-GeV storage ring Aladdin. Synchrotron radiation was dispersed by an extended-range grasshopper monochromator and a 6-m toroidal-grating monochromator which were used for the angle-integrated and angle-resolved measurements, respectively. For the angle-integrated experiments a Leybold EA-10/100 hemispherical analyzer was used while for the angle-resolved experiments a small homemade hemispherical analyzer with a full acceptance angle of 3° was employed. Binding energies were referenced to the Fermi level as measured from a gold foil in electrical contact with the sample. Fermi-level spectra indicated an overall system resolution of 100–200 meV. The STM measurements were performed in one of our vacuum chambers at the University of Illinois with a base pressure 8×10^{-11} Torr. The setup for our STM is described elsewhere.[2]

III. MBE AND HEED

As has been reported previously, the GaSb(100) surface exhibits two types of reconstructions, both sets Sb ter-

minated. For growth temperature $T > 460$ °C, a (1×3), (2×3), or $c(2\times6)$, and $400 > T > 350$ °C a (2×5) or $c(2\times10)$.[3-5] Within each set, the various reconstructions are closely related and the differences may involve subtle details or the degree of disordering. Under the present experimental conditions, we found that the best-quality HEED patterns were generated by first growing a few hundred monolayers of coevaporated Sb and Ga with a deposition ratio of at least 3 to 1, at 500 °C, and then, in the absence of the Ga flux, terminating the surface in the Sb flux in the appropriate temperature range. The evaporation rate for the Sb was 0.16 Å/s. No reconstructions were found under Ga-stabilized conditions. By depositing Ga on any Sb-terminated reconstruction we see only a slow deterioration of the HEED pattern, most likely due to the formation of Ga metallic droplets on the surface.

Stability of the (2×5) or $c(2\times10)$ surface only occurs over a small temperature range and the quality of the HEED pattern was not as high as that for the (1×3) or $c(2\times6)$ surface.[5] For this reason we have concentrated our effort on the high-temperature phase ($T > 460$° C). Contrary to what some other authors observed we never saw a (2×3) reconstruction. Over the many trials, our sample always showed a $c(2\times6)$ HEED pattern. However, the $\frac{1}{2}$ order spots were much weaker than the $\frac{1}{3}$ order spots, in agreement with earlier reports. For simplicity, we will just call our surface a nominal (1×3) surface.

IV. ANGLE-RESOLVED PHOTOEMISSION

We have obtained the valence-band dispersions of GaSb along the [100] direction using angle-resolved photoemission techniques with a wide range of photon energies and a normal-emission geometry. Similar studies along the [110] direction have been reported for the cleaved GaSb(110).[6,7] The technique of band mapping has been described in the literature,[8] and a previous study of the closely related GaAs(100) surfaces prepared by MBE serves as a useful guide for data analysis in the present study.[9] To save space, the readers are referred to these publications for details.

Figures 1 and 2 show a number of normal-emission spectra taken with the photon energies indicated. There is a gap in the photon energy range between the two sets of data shown in the two figures; the spectra taken within the gap are partially obscured by the emission of the Sb $4d$ core level excited by the second-order light from the monochromator and by the Ga and Sb MVV Auger transitions. In the two figures, the peaks labeled $A-C$ and indicated by an inverted triangle are dispersive (the binding energy changes as a function of photon energy), and are derived from direct transitions from the bulk valence bands. Other nondispersive peaks are derived from in-

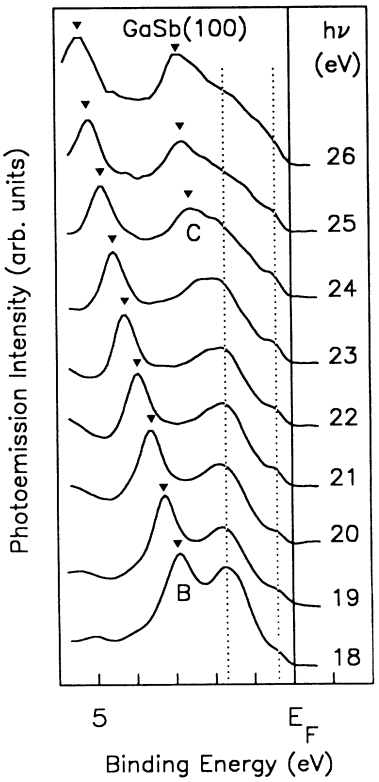

FIG. 1. Normal-emission spectra taken with photon energies between 18 and 26 eV. Binding energies are referenced to the Fermi level E_F. Dispersive peaks, labeled B and C, are indicated by an inverted triangle. Nondispersive peaks are indicated by vertical dotted lines and are located at binding energies of 1.7 and 0.4 eV.

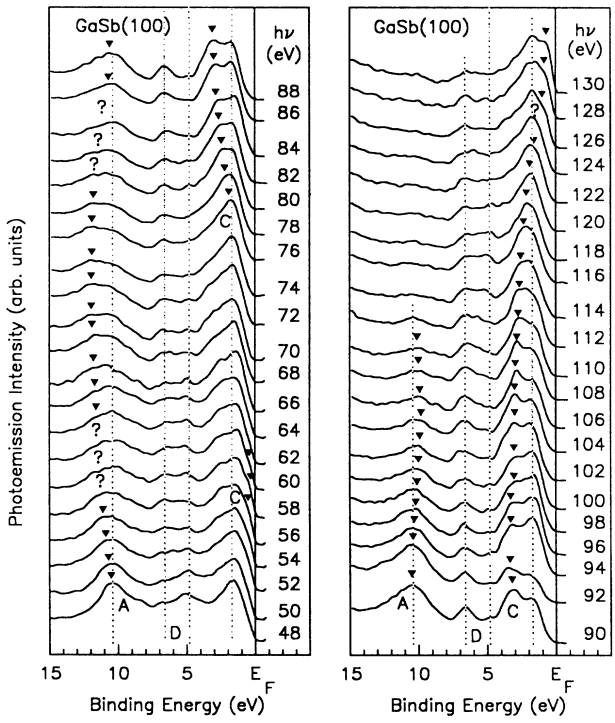

FIG. 2. Photoemission spectra taken with photon energies between 48 and 130 eV. Dispersive peaks, labeled A and C, are indicated by an inverted triangle. Question marks indicate a dispersive-peak position difficult to determine due to an obscuring nondispersive peak. Nondispersive peaks are indicated by vertical dotted lines and are located at binding energies of 10.4, 6.6, 4.8, and 1.7 eV. The peak located at 6.6 eV is labeled D.

direct transitions and represent density-of-state features or surface states. The major nondispersive peaks are indicated by vertical dotted lines. In some of the spectra the dispersive peaks merge with one or more nondispersive peaks at binding energies of 10.4, 6.6, 4.8, and 1.7 eV. Because of this inconvenience, certain dispersive-peak positions were difficult to determine and consequently were labeled with a question mark. Uncertainties in the peak positions as marked by the triangles in the figures are, in general, less than about 0.2 eV.

As in previous band mapping studies, we assume a free-electron dispersion for the final band. The component of the crystal momentum parallel to the surface is zero because of the normal-emission geometry. The perpendicular component is given by

$$\hbar k_{\perp}=[2m(h\nu-E_B-V_0)]^{1/2}\ , \tag{1}$$

where $h\nu$ is the incident photon energy, E_B is the binding energy (a positive quantity), and V_0 is the inner potential (taken to be -7.2 eV referred to the Fermi level).[7] Using Eq. (1) and the measured peak positions, we plot the experimental and theoretically predicted band dispersions in Fig. 3. The theoretical predictions are plotted as solid curves and were calculated using a nonlocal empirical pseudopotential method.[10] The experimental peak points are shown as diamonds, squares, triangles, and circles which denote momenta in the extended-zone scheme for different zones, namely $2k_{\Gamma\Delta X}<k_{\perp}<3k_{\Gamma\Delta X}$, $3k_{\Gamma\Delta X}<k_{\perp}<4k_{\Gamma\Delta X}$, $4k_{\Gamma\Delta X}<k_{\perp}<5k_{\Gamma\Delta X}$, and $5k_{\Gamma\Delta X}<k_{\perp}<6k_{\Gamma\Delta X}$. The inverted triangle located at X_6 is an assignment based on the energy position of the nondispersive peak D in Fig. 2.[7-9] A typical uncertainty for each data point is shown where the uncertainty in momentum is typically less than 10% of the Brillouin-zone size.[8] The data were plotted with the valence-band maximum at E_V as the energy reference for easy comparison to theory. We determined $E_F-E_V=0.25\pm0.10$ eV from the energy difference between the Fermi level and the onset of emission in a number of angle-integrated valence-band spectra which are not shown, and the average value of 0.25 eV was used in converting the energy references. Figure 3 shows that the theoretical and experimental results are in reasonable agreement.

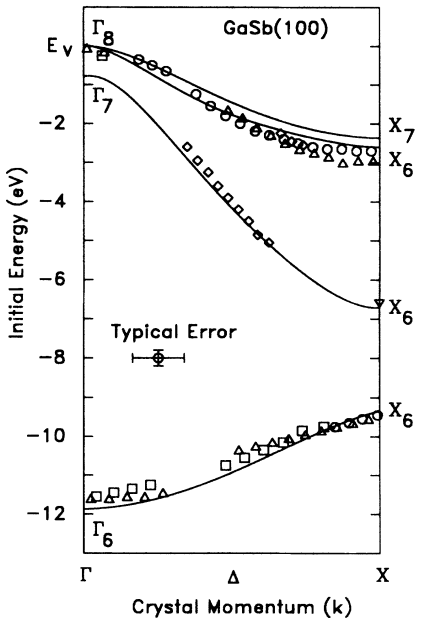

FIG. 3. Band dispersions for GaSb(100) along Γ-Δ-X. Initial energies are referenced to the valence-band maximum. The experimental peak points are shown as diamonds, squares, triangles, and circles which denote crystal momenta in the extended-zone scheme for different zones, namely $2k_{\Gamma\Delta X}<k_{\perp}<3k_{\Gamma\Delta X}$, $3k_{\Gamma\Delta X}<k_{\perp}<4k_{\Gamma\Delta X}$, $4k_{\Gamma\Delta X}<k_{\perp}<5k_{\Gamma\Delta X}$, and $5k_{\Gamma\Delta X}<k_{\perp}<6k_{\Gamma\Delta X}$. The inverted triangle located at X_6 is an assignment based on the energy position of the nondispersive peak D in Fig. 2. Typical uncertainties in the energy and momenta are indicated. The theoretical band dispersions are plotted as solid curves. Critical points are shown in their relativistic notation.

V. ANGLE-INTEGRATED PHOTOEMISSION

A. Clean-surface results

Figure 4 shows two representative spectra of the Sb 4d core level of GaSb(100)-(1×3) recorded using two different photon energies. The 75-eV spectrum is much more surface sensitive than the 55-eV spectrum because of escape-depth considerations. There is obvious filling in

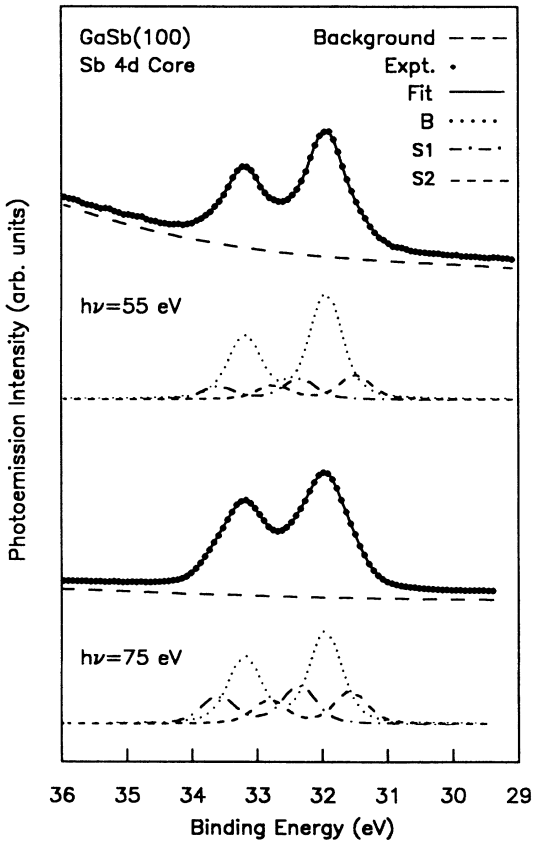

FIG. 4. The Sb 4d core-level spectra (dots) with the decomposition of the spectra into background (long-dashed curve), bulk (dotted curve), and two surface contributions (short-dashed and dot-dashed curves). The binding-energy scale is referred to the Fermi level.

in between the doublet and the lower and higher binding-energy side of the surface-sensitive spectrum, indicating at least two surface-shifted core-level components, one at higher and the other at lower binding energies relative to the bulk component. This is consistent with a previous observation.[11] To determine the surface shifts and the intensities of the various components, we follow the fitting procedure described previously.[11–13] The fit involves a bulk and surface-shifted components, each represented by a spin-orbit-split doublet, riding on a cubic polynomial background. The doublet was modeled by the sum of two Voigt functions (a convolution of a Gaussian with a Lorentzian). In these fits the Lorentzian width, spin-orbit splitting, and intensity branching ratio between the $d_{3/2}$ and the $d_{5/2}$ contributions were constrained to be the same between the surface-shifted components and the bulk. In the first try, only one surface-shifted component was assumed, representing the simplest possible case, but the spectra could not be reasonably fit. Not only did the intensity of the surface-shifted component change randomly but also the energy shift moved around quite randomly as a function of photon energy. In general, the quality of the fit was poor. Excellent fits were obtained if two surface shifts were assumed. The experimental results (dots), the overall fit (solid curve), the background (long-dashed curve), the bulk component B (dotted curve), and the two surface components $S1$ and $S2$ (dot-dashed and short-dashed curves) are shown in Fig. 4. The binding energies are referenced to the Fermi level.

Since the line shape does not show distinct features due to the surface shifts, it is important to check the reliability of the fitting procedure. We have fitted the line shapes obtained with many photon energies between 55 and 100 eV following the exact same procedure. The two surface shifts remain constant within tight tolerances ($S1$ shift was -0.41 ± 0.01 eV and $S2$ shift was 0.40 ± 0.02 eV), and the intensities relative to the bulk emission do follow the expected behavior based on escape-depth considerations. Figure 5 summarizes the results of this analysis. The intensity ratios of the two surface components and the bulk component are plotted as a function of photon energy. Both ratios are seen to evolve in basically the same fashion, and go through a maximum around $h\nu=75-80$ eV. These ratios reflect the escape depth of the electrons ejected from the solid in the near-surface region. The observed behavior is consistent with not only the universal mean-free-path curve but also a similar curve for the Sb core level in InSb(100)-$c(4\times4)$.[14,15] These results strongly suggest the validity of the basic fitting assumptions. The fitting parameters are summarized in Table I.

The Ga $3d$ core-level line shape has been similarly analyzed. Figure 6 shows two typical spectra together with the fit and the decomposition. The 55-eV spectrum is more surface sensitive than the 40-eV spectrum. Again, two surface components are found. The fitting parameters are given in Table I.

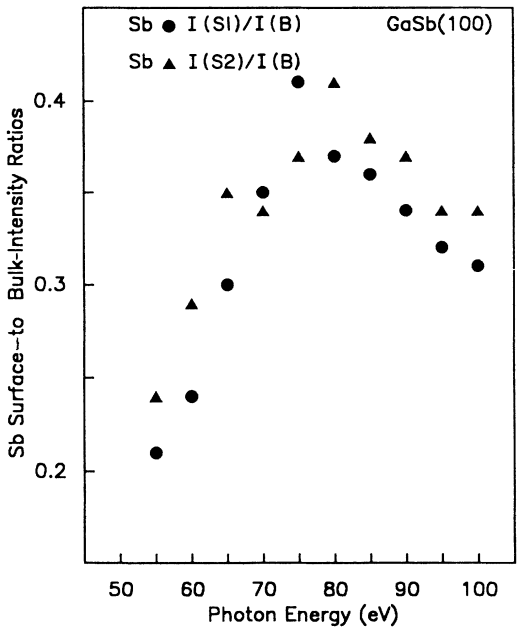

FIG. 5. The Sb surface- to bulk-photoemission-intensity ratios for GaSb(100)-(1×3) as a function of photon energy. Circles and triangles indicate the results for the $S1$ and $S2$ component, respectively.

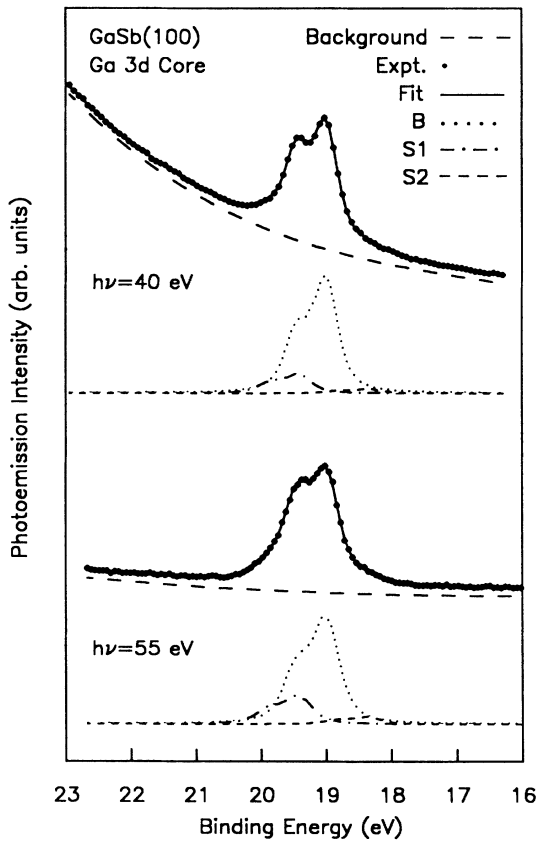

FIG. 6. The Ga $3d$ core-level spectra (dots) with the decomposition of the spectra into background (long-dashed curve), bulk (dotted curve), and two surface contributions (short-dashed and dot-dashed curves). The binding-energy scale is referred to the Fermi level.

TABLE I. Fitting parameters for the Sb 4*d* and Ga 3*d* core-level data. All energies are in eV. Binding energies for the Sb $4d_{5/2}$ and Ga $3d_{5/2}$ are referenced to the Fermi level. All energy-independent parameters were computed from many spectra and are listed below as an average and its variation. Typical values of the branching ratio, Gaussian width, and surface- to bulk-intensity ratios are shown using photon energies of 75 and 55 eV for the Sb 4*d* and Ga 3*d* core levels, respectively. The widths refer to full width at half maximum.

	Sb	Ga
Binding energy	31.94	19.00
Spin-orbit splitting	1.25±0.01	0.45±0.01
Branching ratio	1.43	1.78
Gaussian width	0.45	0.38
Lorentzian width	0.24±0.02	0.26±0.03
$S1$ surface shift	−0.41±0.01	−0.43±0.03
$I(S1)/I(B)$ intensity ratio	0.41±0.02	0.24±0.02
$S2$ surface shift	0.40±0.02	0.66±0.03
$I(S2)/I(B)$ intensity ratio	0.37±0.02	0.07±0.02

B. Ga-deposition results

We deposited various submonolayer coverages of Ga onto the GaSb(100)-(1×3) at room temperature and then, after annealing the surface for 3 min at 500 °C, examined the surfaces with core-level photoemission. Figures 7 and 8 show stack plots of our results. Each spectrum was fitted in the exact manner we used for the clean spectrum. Table II shows the surface- to bulk-intensity ratios as a function of Ga coverages for the Sb 4*d* taken at 75 eV and the Ga 3*d* taken at 55 eV. All results show no change in either the Sb or Ga core-level line shapes, within uncertainty. HEED was used after each growth to monitor surface changes; here too, no significant changes were noted in the diffraction patterns.

C. Core-level analysis and structural model

The core-level results of the preceding section can be interpreted as deposited Ga balling up in droplets on the surface. A similar effect has been seen in our previous experiments with GaAs(100); the metallic Ga droplets could, in fact, be observed directly with an optical microscope for a sufficient amount of excess Ga on the surface. Since the actual surface area covered by these metallic droplets is small they would account for a small part of the photoemission spectra. Photoemission from the Ga core of the metallic droplets on GaAs(100) was found to have a lower binding energy than the bulk GaAs contribution, similar to the $S2$ component seen in Fig. 6. The Ga balling-up effect has also been reported for the growth of GaAs on Si, and a lower binding-energy component

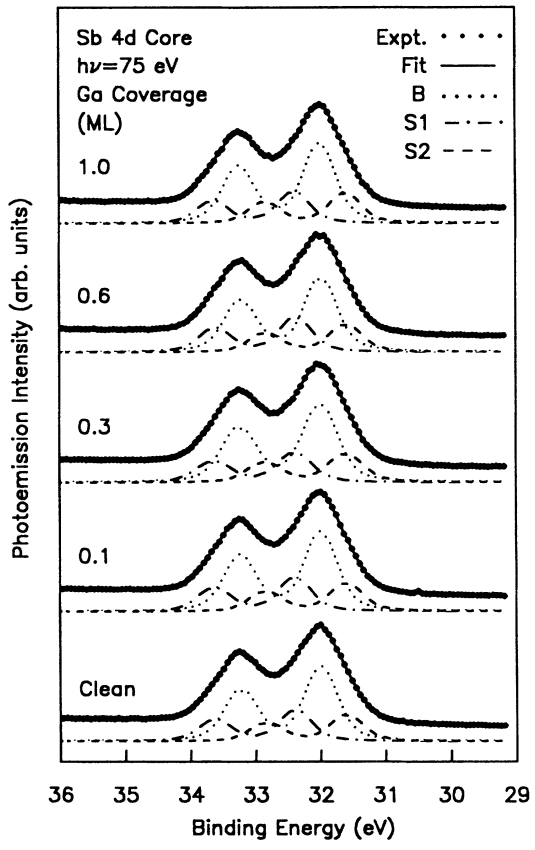

FIG. 7. Sb 4*d* core-level spectra (dots) taken with a photon energy of 75 eV. The Ga coverages are indicated. The solid curves are a result of a fit to the data. The decomposition of the spectra into bulk, *B*, and surface contributions, $S1$ and $S2$, are shown by the various curves.

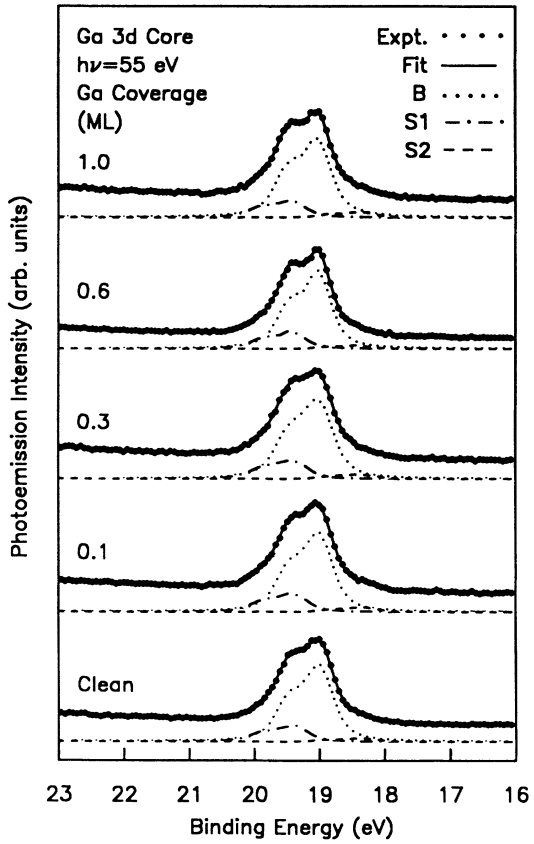

FIG. 8. Ga 3*d* core-level spectra (dots) taken with a photon energy of 55 eV. The Ga coverages are indicated. The solid curves are a result of a fit to the data. The decomposition of the spectra into bulk, *B*, and surface contributions, $S1$ and $S2$, are shown by the various curves.

TABLE II. Surface- to bulk-intensity ratios for the Sb 4*d* and the Ga 3*d* core levels as a function of Ga coverage. All ratios are uncertain by about ±0.02. Note that Table I shows the average clean-surface ratios for Sb and Ga.

Ga coverage	Sb		Ga	
(ML)	$I(S1)/I(B)$	$I(S2)/I(B)$	$I(S1)/I(B)$	$I(S2)/I(B)$
clean	0.43	0.37	0.22	0.05
0.1	0.43	0.36	0.24	0.06
0.3	0.39	0.37	0.23	0.06
0.6	0.44	0.33	0.24	0.05
1.0	0.40	0.38	0.22	0.07

was correspondingly observed.[16] Based on these results, we assign the very weak $S2$ component in the Ga core-level spectra to be derived from metallic Ga droplets on the surface. The droplets would affect the HEED in an increase in the background; in our experiment described in the preceding section, the amount of Ga deposited was too small to have any observable effect. In the following analysis, we will ignore this very weak component in the Ga core-level spectra.

The GaSb(100)-(1×3) surface is Sb terminated due to the nature of the preparation procedure. We also used Auger spectroscopy and found that the intensity ratio between the Sb Auger transition at 454 eV and the Ga transition at 1070 eV increased by a factor of approximately 1.5 between the sputtered-only surface and the fully grown (1×3) surface; indicating the enrichment of the surface with Sb.

Information about the surface structure and stoichiometry is revealed by the two surface components in the Sb 4*d* core-level spectra. The intensities of the two components are about the same, indicating the presence of two surface Sb species with about equal coverage. The Ga core-level results indicate the presence of one surface species (ignoring the metallic droplets). Since the $I(S1)/I(B)$ intensity ratio for the Ga core level at the escape-depth minimum ($h\nu \approx 55$ eV) is about $\frac{1}{2}$ that of the Sb ($h\nu \approx 75$ eV), the surface Ga coverage is about $\frac{1}{2}$ of that of either Sb surface species. To analyze these results further we use the standard layer attenuation model. We assume a fraction of monolayer f of Ga terminating the surface giving rise to the $S1$ component; the intensity of the surface contribution is then

$$I_S = fI \ , \tag{2}$$

where I is intensity for a full monolayer of Ga on the surface. The bulk contribution has an intensity

$$I_B = I[\exp(-2d/l) + \exp(-4d/l) + \cdots] \ , \tag{3}$$

where d is the interlayer spacing of 1.52 Å and l is the escape depth. Combining Eqs. (2) and (3) we find

$$f = (I_S/I_B)[\exp(-2d/l) + \exp(-4d/l) + \cdots] \ . \tag{4}$$

The escape depth minimum is about 5.5 Å based on previous studies of InSb(100) and GaAs(100).[15,17] Taking $l = 5.5 \pm 0.5$ Å and using the measured value of $I_S/I_B = 0.24$, we obtain $f = 0.33 \pm 0.04$. This indicates that approximately $\frac{1}{3}$ ML of Ga is on the surface. This $\frac{1}{3}$ ML coverage ties in well with the (1×3) reconstruction. The coverage for each of the two surface species of Sb is thus about $\frac{2}{3}$ ML.

Based on the above coverages of the various surface species, we propose the model shown in Fig. 9 for the (1×3) reconstruction. The model incorporates an important structural ingredient previously proposed for the group-V enriched surfaces of GaAs(100)-c(4×4) (Refs. 17 and 18) and InSb(100)-c(4×4) (Ref. 15) which is Sb dimers bonded on top of an Sb layer. Note that the bulk structure of GaSb(100) consists of alternating layers of Ga and Sb square nets. The easiest way to view the (1×3) model is to consider a unreconstructed Ga-terminated surface with two of every three Ga rows along the $[01\bar{1}]$ direction on the surface replaced by Sb rows and allow the neighboring Sb atoms to form dimers to

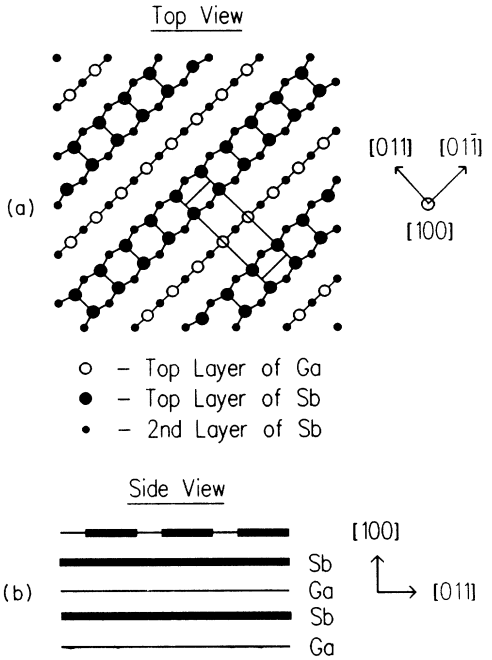

FIG. 9. A structural model for GaSb(100)-(1×3) showing (a) the top view, and (b) the side view. The top view shows the first two layers of the surface with the (1×3) unit cell indicated. Sb (Ga) atoms on the top layer are indicated by large solid (open) circles while Sb atoms on the second layer are indicated by small closed circles.

minimize the number of dangling bonds. In this model, there is $\frac{1}{3}$ ML of twofold-coordinated Ga left on the surface, accounting for the $S1$ component seen in the core-level spectra. The model also shows $\frac{2}{3}$ ML of Sb on the top layer, each atom is threefold coordinated, which should correspond to one of the two surface shifts. In the second layer (the layer just below the surface layer), $\frac{2}{3}$ ML of Sb are bonded to surface Sb dimers; each of these Sb atoms is bonded to two surface Sb dimer atoms and two third-layer Ga atoms. A core-level shift is expected for these Sb atoms, since the bonding environment is different from that in the bulk in which each Sb atom is bonded to four Ga atoms. The remaining $\frac{1}{3}$ ML of Sb in the second layer should exhibit a bulklike core-level binding energy, because each of these Sb atoms is bonded to four Ga atoms as in the bulk. This model thus explains the photoemission intensities of all of the surface-shifted components. There remains the question as to which surface shift corresponds to which kind of Sb atoms. The problem of determining surface shifts is a complicated matter requiring a detailed calculation based on the exact atomic structure which is lacking in the present case. In general, the surface shift depends on not only the local electronic and atomic structure but also the long-range electrostatic interaction.[13,19] However, based on the similar results of previous studies of InSb(100)-$c(4\times4)$ and GaAs(100)-$c(4\times4)$, in which group-V adatoms on top of a group-V atomic layer are associated with a higher core-level binding energy, we assign the $S1$ ($S2$) component in Fig. 4 to be derived from the $\frac{2}{3}$ ML of Sb atoms in the top (second) layer.

VI. STM

Our clearest topographs showing the most detail were obtained with a sample bias voltage between -30 and -125 mV relative to the tip and a constant tunneling current typically between 0.2 and 0.6 nA. Figure 10 shows a typical STM grey-scale image, where bright areas represent protrusions. Due to the lack of an adequate grey-scale range for a proper presentation on paper, the low spatial frequencies in the image have been filtered out in the data to emphasize the local height variations. As a result of the filtering, terraces separated by steps appear equally bright, even though the steps can still be recognized. There is one step in Fig. 10 as indicated. The x-y scale of the image is somewhat distorted by a uniform thermal drift during the data taking. The picture shows bright strips along the $[01\bar{1}]$ direction separated by about 13 Å, suggesting that these correspond to the Sb dimer rows shown in Fig. 9. Since each Sb atom on the surface is only threefold coordinated, we expect a lone-pair orbital pointing out of the surface, which should contain substantial occupied density of states visible with a negative bias. Notice that the dimer rows are not perfectly straight and uniform as in the case of Si(100)-(2×1) observed under similar conditions, indicating the presence of disorder.[20,21]

To view the detail, the part of Fig. 10 enclosed in the rectangle is magnified and shown in Fig. 11. The picture clearly shows dimerlike structures with the measured

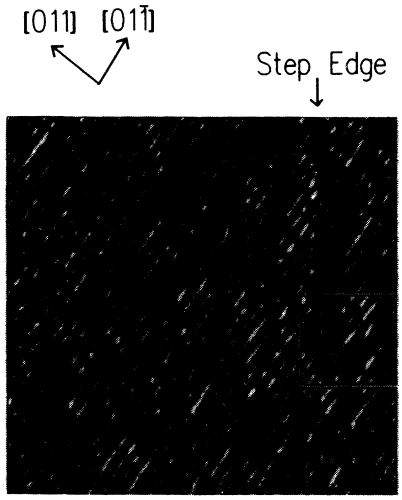

FIG. 10. A typical STM image of GaSb(100)-(1×3) taken over an area of about 560×450 Å. A sample bias of -30 mV and a tunneling current of 0.3 nA were used. An atomic step is seen in the right-hand portion of the image. A box outlines the area that will be magnified for Fig. 11.

dimer-dimer spacings corresponding closely to the expected values. Also evident is the partial disorder in the form of fluctuations in height and lateral registry. As with the GaAs(100) surface previously studied with STM, disorder seems to play a large role on this surface.[22,23] Over the many trials, we always observed the same kind of disorder on this surface, and therefore, we believe that the disorder is intrinsic to this structure. Despite the disorder, the surface shows relatively unbroken dimerized rows of the (1×3) unit cell.

According to the model shown in Fig. 9, there is a row

FIG. 11. This image is from the magnified portion of the box in Fig. 10. The image size is about 140×110 Å.

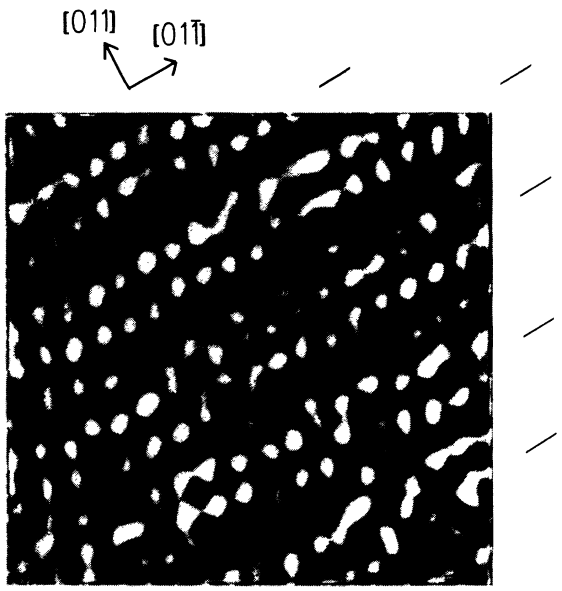

FIG. 12. A higher resolution STM image of the GaSb(100)-(1×3) surface taken over an area of about 50×70 Å with a sample bias of −125 mV and a tunneling current of 0.6 nA. Tic marks indicate the dimer rows which, due to disorder, fluctuate in height and lateral registry.

of Ga atoms in between two neighboring Sb dimer rows. Each of these Ga atoms possesses a dangling bond which should also be visible with STM, although the apparent height in the STM picture is likely to be less due to the half filled nature of the bond. Figure 12 is a smaller scan with higher resolution. The grey scale has been renormalized to bring out further details between the Sb dimer rows which are labeled by tic marks on the side of the picture. Indeed, we observe an additional protrusion in between many of neighboring dimer pairs, and the position does correspond to the model. This picture also shows more clearly the disorder and defects of the structure. When an Sb dimer row meanders toward its neighboring row, the Ga atom in between is not observed, perhaps simply due to spatial-resolution problems. On the other hand, it is also possible that some of the surface Sb atoms actually form bonds with neighboring surface Ga atoms causing the Sb row to shift in its lateral registry. The disorder could also be induced by intrinsic strain.[24] We do not have the answer to this question and hope that theorists will be able to help.

The STM pictures clearly show the overall (1×3) reconstruction, but we are not able to detect the $c(2\times6)$ superstructure by visual inspection. This implies that the larger reconstruction is rather weak, perhaps involving only minute modulation of either atomic height or lateral position on top of the basic (1×3) structure. This is consistent with our HEED observation that the $\frac{1}{2}$ order spots are much weaker than the $\frac{1}{3}$ order spots.

It is interesting to compare the present STM results with those reported on the GaAs(100)-$c(2\times8)$ or -(2×4) surface.[23] The topographs appear qualitatively different in that the present results show individual dimer atoms clearly while the GaAs results show only patches formed by unresolved trios of neighboring dimers bordered by missing dimers.

VII. SUMMARY

We have obtained the bulk band structure of GaSb along the [100] direction with the use of angle-resolved photoemission. The results are in fairly good agreement with theory. Through the use of MBE, HEED, core-level spectroscopy, and STM the structure of the GaSb(100)-(1×3) surface is investigated. A structural model is proposed, which can consistently explain all of the essential features of the experimental results. We observed significant disorder on this surface; the origin of this awaits a theoretical explanation.

ACKNOWLEDGMENTS

This material is based upon work supported by the U.S. Department of Energy (Division of Materials Sciences, Office of Basic Energy Sciences), under Contract No. DE-AC02-76ER01198. Some of the personnel and equipment support was also derived from grants from the U.S. National Science Foundation (Grant No. DMR-83-52083 and No. DMR-86-14234) and the E.I. du Pont de Nemours and Company (Wilmington, DE). We acknowledge the use of central facilities of the Materials Research Laboratory of the University of Illinois, which was supported by the U.S. Department of Energy (Division of Materials Sciences, Office of Basic Energy Sciences), under Contract No. DE-AC02-76ER01198, and the U.S. National Science Foundation under Contract No. DMR-83-16981.

[1]H. C. Casey and M. B. Panish, *Heterostructure Lasers* (Academic, New York, 1978).
[2]F. M. Leibsle, A. Samsavar, and T.-C. Chiang, Phys. Rev. B **38**, 5780 (1988).
[3]R. Ludeke, IBM J. Res. Dev. **22**, 304 (1978).
[4]A. J. Van Bommel and J. E. Crombeen, Surf. Sci. **93**, 383 (1980).
[5]T. H. Chiu and W. T. Tsang, J. Appl. Phys. **57**, 4572 (1985).
[6]Gwyn P. Williams, F. Cerrina, G. J. Lapeyre, J. R. Anderson, R. J. Smith, and J. Hermanson, Phys. Rev. B **34**, 5548 (1986).
[7]T.-C. Chiang and D. E. Eastman, Phys. Rev. B **22**, 2940 (1980).
[8]T.-C. Chiang, J. A. Knapp, M. Aono, and D. E. Eastman, Phys. Rev. B **21**, 3513 (1980).
[9]T.-C. Chiang, R. Ludeke, M. Aono, G. Landgren, F. J. Himpsel, and D. E. Eastman, Phys. Rev. B **27**, 4770 (1983).
[10]J. R. Chelikowsky and M. L. Cohen, Phys. Rev. B **14**, 556 (1976).
[11]R. Ludeke, T.-C. Chiang, and D. E. Eastman, Physica B+C (Amsterdam) **117&118B**, 819 (1983).
[12]T. Miller, F. Rosenwinkel, and T.-C. Chiang, Solid State

Commun. **47**, 935 (1983); Phys. Rev. B **30**, 570 (1984).
[13]T.-C. Chiang, CRC Crit. Rev. Solid State Mater. Sci. **14**, 269 (1988).
[14]C. R. Brundle, J. Vac. Sci. Technol. **11**, 212 (1974).
[15]P. John, T. Miller, and T.-C. Chiang, Phys. Rev. B **39**, 1730 (1989).
[16]R. D. Brigans, M. A. Olmstead, R. I. G. Uhrberg, and R. Z. Bachrach, Phys. Rev. B **36**, 9569 (1987).
[17]J. F. van der Veen, P. K. Larsen, J. H. Neave and B. A. Joyce, Solid State Commun. **49**, 659 (1984).
[18]P. K. Larsen, J. H. Neave, J. F. van der Veen, P. J. Dobson, and B. A. Joyce, Phys. Rev. B **27**, 4966 (1983).
[19]R. E. Watson, J. W. Davenport, M. L. Perlman, and T. K. Sham, Phys. Rev. B **24**, 1791 (1981).
[20]R. M. Tromp, R. J. Hamers, and J. E. Demuth, Phys. Rev. Lett. **55**, 1303 (1985).
[21]A. Samsavar, E. S. Hirschorn, F. M. Leibsle, and T.-C. Chiang, Phys. Rev. Lett. **63**, 2830 (1989).
[22]M. D. Pashley, K. W. Haberern, and J. M. Woodall, J. Vac. Sci. Technol. B **6**, 1468 (1988).
[23]M. D. Pashley, K. W. Haberern, W. Friday, J. M. Woodall, and P. D. Kirchner, Phys. Rev. Lett. **60**, 2176 (1988); D. K. Biegelsen, L.-E. Swartz, and R. D. Bringans, J. Vac. Sci. Technol. A **8**, 280 (1990); D. K. Biegelsen, R. D. Bringans, J. E. Northrup, and L.-E. Swartz, Phys. Rev. B **41**, 5701 (1990).
[24]J. E. Demuth, U. K. Koehler, R. J. Hamers, and P. Kaplan, Phys. Rev. Lett. **62**, 641 (1989).

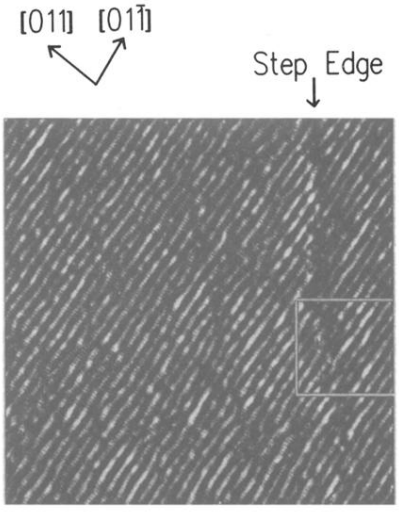

FIG. 10. A typical STM image of GaSb(100)-(1×3) taken over an area of about 560×450 Å. A sample bias of −30 mV and a tunneling current of 0.3 nA were used. An atomic step is seen in the right-hand portion of the image. A box outlines the area that will be magnified for Fig. 11.

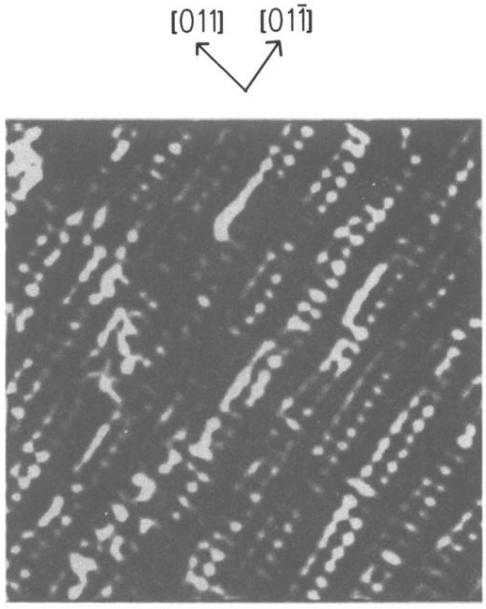

FIG. 11. This image is from the magnified portion of the box in Fig. 10. The image size is about 140×110 Å.

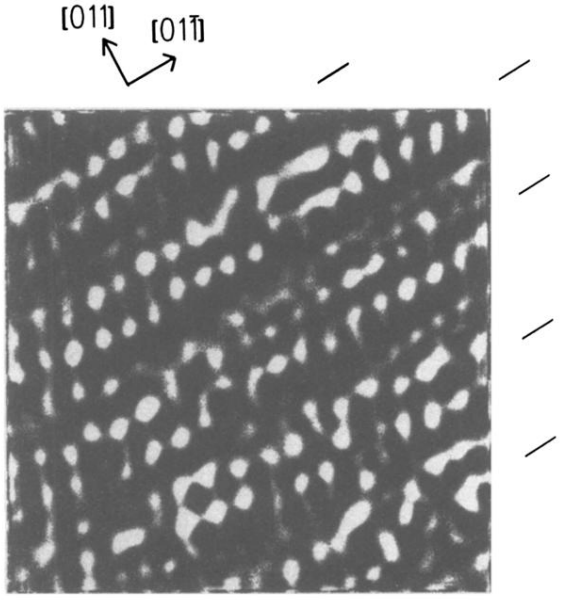

FIG. 12. A higher resolution STM image of the GaSb(100)-(1×3) surface taken over an area of about 50×70 Å with a sample bias of −125 mV and a tunneling current of 0.6 nA. Tic marks indicate the dimer rows which, due to disorder, fluctuate in height and lateral registry.